

FIG. 1. Relationship between the true and reconstructed muon energy in the IceCube MC sample [4]. Shaded area shows the 99.9th percentile limits predicted by the regressor trained on this set.

I. METHODOLOGY

The neutrino flux at the detector is calculated by propagating the atmospheric neutrino flux [1] through the Earth by solving the Schrödinger equation for varying density. The Earth density profile is taken from the PREM [2]. The oscillation probability $P_{\alpha\beta}$ then acts as a weight, yielding the propagated flux at detector level for flavor β as

$$\phi_{\beta}^{\text{det}} = \sum_{\alpha} \frac{d^2 \phi_{\alpha}^{\text{atm}}}{dE^t d \cos \theta_z^t} P_{\alpha\beta}, \quad (1)$$

where we sum over the initial lepton flavors $\alpha \in \{e, \mu, \bar{e}, \bar{\mu}\}$.

A. IceCube

The event rate for each bin reads

$$N_{ij} = T \int_{(\cos \theta_z^r)_i}^{(\cos \theta_z^r)_{i+1}} d \cos \theta_z^r \int_{E_j^r}^{E_{j+1}^r} dE^r \int_0^{\pi} R(\theta^r, \theta^t) d \cos \theta^t \int_0^{\infty} R(E^r, E^t) dE^t \times \left[\sum_{\beta} \phi_{\beta}^{\text{det}} A_{\beta}^{\text{eff}} \right], \quad (2)$$

where T is the live time of the detector, and A_{β}^{eff} its effective area for flavor β . We use the effective area of the 86 string configuration made public by the IceCube collaboration [3]. $R(x^r, x^t)$ is a Gaussian resolution function, which is responsible for the smearing between the reconstructed and true parameters x^r and x^t , respectively. It takes the form

$$R(x^r, x^t) = \frac{1}{\sqrt{2\pi}\sigma_{x^r}} \exp \left[-\frac{(x^r - \mu(x^t))^2}{2\sigma_{x^r}^2} \right]. \quad (3)$$

Assuming no bias in the reconstruction, the mean of the Gaussian can be taken as $\mu(x^t) = x^t$. As seen in Fig. 1, the distribution of simulated events is skewed. Instead, we assume a log-normal distribution between E^{true} and E^{reco} , and train a Gaussian Process Regressor on the dataset [4], from which we can extract a predicted mean and standard deviation for each E^{reco} . We then sample values from this distribution to yield the points of E^{true} at which to integrate over.

In Icecube, the zenith angle resolution for track-like events is less than 2° , making $\cos(\theta_z^{\text{true}})$ coincide with $\cos(\theta_z^{\text{reco}})$ for our study [5]. The data is from the IC86 sterile analysis [5].

B. DeepCore

In this part, we use the publically available DeepCore data sample [6] which is an updated version of what was used by the IceCube collaboration in an ν_μ disappearance analysis [7].

The detector systematics include ice absorption and scattering, and overall, lateral, and head-on optical efficiencies of the DOMs. They are applied as correction factors using the best-fit points from the DeepCore 2019 ν_τ appearance analysis [8].

The data include 14901 track-live events and 26001 cascade-like events, both divided into eight $\log_{10} E^{reco} \in [0.75, 1.75]$ bins, and eight $\cos(\theta_z^{reco}) \in [-1, 1]$ bins.

The oscillation parameters are from the best-fit in the global analysis in [9]: $\theta_{12} = 33.44^\circ$, $\theta_{13} = 8.57^\circ$, $\Delta m_{21}^2 = 7.42 \text{ eV}^2$, and we marginalize over Δm_{31}^2 and θ_{23} .

Given a Monte Carlo simulation with weights $w_{k\beta}$, we can construct the event count as

$$N_{ijk} = C_{ijk} \sum_{\beta} w_{ijk,\beta} \phi_{\beta}^{\text{det}}, \quad (4)$$

where $C_{k\beta}$ is the correction factor from the detector systematic uncertainty and $\phi_{\beta}^{\text{det}}$ is defined as Eq. 1. We have now substituted the effect of the Gaussian smearing by treating the reconstructed and true quantities as a migration matrix.

C. PINGU

The methodology behind the PINGU simulations are the same as with our DeepCore study IB. We use the public MC [10], which allows us to construct the event count as in Eq. 4. As with the DeepCore data, the PINGU MC is divided into eight $\log_{10} E^{reco} \in [0.75, 1.75]$ bins, and eight $\cos(\theta_z^{reco}) \in [-1, 1]$ bins for both track- and cascade-like events. We generate "data" by predicting the event rates at PINGU with the following best-fit parameters from [9], except for the CP-violating phase which is set to zero for simplicity.

$$\begin{aligned} \Delta m_{21}^2 &= 7.42 \times 10^{-5} \text{ eV}^2, \quad \Delta m_{31}^2 = 2.517 \times 10^{-3} \text{ eV}^2, \\ \theta_{12} &= 33.44^\circ, \quad \theta_{13} = 8.57^\circ, \quad \theta_{23} = 49.2^\circ, \quad \delta_{\text{CP}} = 0. \end{aligned} \quad (5)$$

II. RESULTS

For our analyses, we define our χ^2 as

$$\chi^2(\hat{\theta}, \alpha, \beta, \kappa) = \sum_{ijk} \frac{(N^{\text{th}} - N^{\text{data}})_{ijk}^2}{\left(\sigma_{ijk}^{\text{data}}\right)^2 + \left(\sigma_{ijk}^{\text{syst}}\right)^2} + \frac{(1 - \alpha)^2}{\sigma_{\alpha}^2} + \frac{\beta^2}{\sigma_{\beta}^2} \quad (6)$$

where we minimize over the model parameters $\hat{\theta} \in \{\Delta m_{31}^2, \theta_{23}, \epsilon', \epsilon_{\mu\tau}\}$, the penalty terms α and β , and the free parameter κ . N_{ijk}^{th} is the expected number of events from theory, and N_{ijk}^{data} is the observed number of events in that bin. We set $\sigma_{\alpha} = 0.25$ as the atmospheric flux normalization error, and $\sigma_{\beta} = 0.04$ as the zenith angle slope error [1]. The observed event number has an associated Poissonian uncertainty $\sigma_{ijk}^{\text{data}} = \sqrt{N_{ijk}^{\text{data}}}$.

For IceCube, the event count takes the form

$$N_{ijk}^{\text{th}} = \alpha [1 + \beta(0.5 + \cos(\theta_z^{reco})_i)] N_{ijk}(\hat{\theta}), \quad (7)$$

with $N_{ijk}(\hat{\theta})$ from Eq. 2. Here, we allow the event distribution to rotate around the median zenith of -0.5 .

For DeepCore and PINGU, the event count takes the form

$$N_{ijk}^{\text{th}} = \alpha [1 + \beta \cos(\theta_z^{reco})_i] N_{ijk}(\hat{\theta}) + \kappa N_{ijk}^{\mu atm}, \quad (8)$$

with $N_{ijk}(\hat{\theta})$ from Eq. 4. $N_{ijk}^{\mu atm}$ is the muon background, which is left to float freely in the DeepCore analysis. The background at PINGU can be considered negligible to first order [10], and we thus put $\kappa = 0$ when calculating the

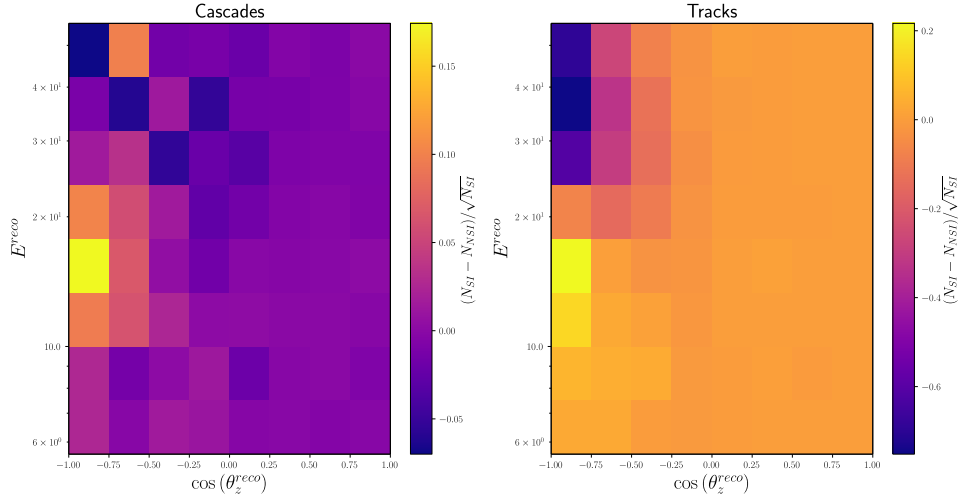


FIG. 2. Expected pulls of predicted event numbers for DeepCore. We compare the NSI event count with $\epsilon_{\mu\tau} = -0.05$ to the standard interaction count

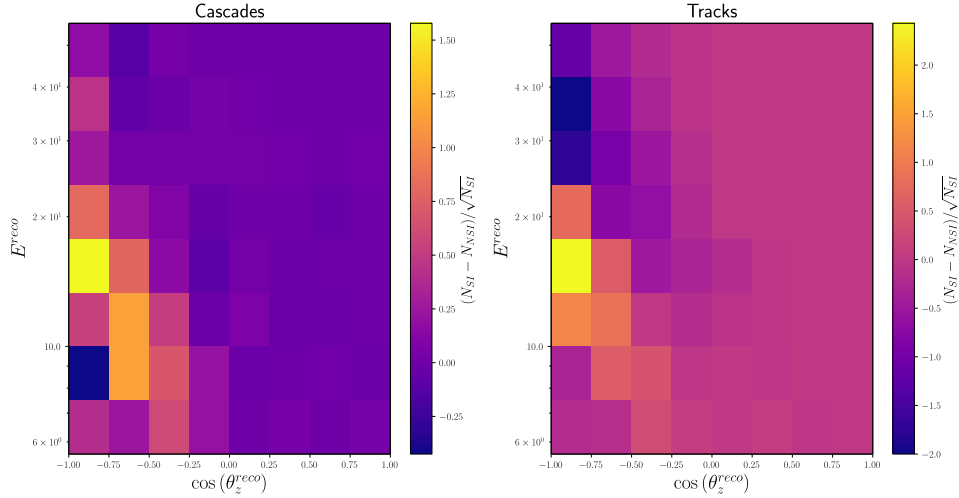


FIG. 3. Expected pulls of predicted event numbers for PINGU. We compare the NSI event count with $\epsilon_{\mu\tau} = -0.05$ to the standard interaction count

PINGU χ^2 . For IceCube, we set $\sigma_{ijk}^{\text{syst}} = f\sqrt{N_{ijk}^{\text{data}}}$. For DeepCore, we use the provided systematic error distribution which accounts for both uncertainties in the finite MC statistics and in the data-driven muon background estimate [6].

We plot the event pull $(N_{NSI} - N_{SI})/\sqrt{N_{SI}}$ where $N_{(N)SI}$ are the numbers of expected events assuming (non-)standard interactions. This gives the normalized difference in the number of expected events at the detector, and illustrates the expected sensitivity for the NSI parameters.

For the joint analysis, we follow the parameter goodness-of-fit prescription [12] and construnt the joint χ^2 as

$$\chi_{joint}^2 = \chi_{IC}^2 + \chi_{DC}^2 + \chi_P^2 - \chi_{IC,min}^2 + \chi_{DC,min}^2 + \chi_{P,min}^2 \quad (9)$$

with test statistic $\chi_{joint,min}^2$.

[1] M. Honda et al., Calculation of atmospheric neutrino flux using the interaction model calibrated with atmospheric muon data.[doi:10.1103/PhysRevD.75.043006](https://doi.org/10.1103/PhysRevD.75.043006).

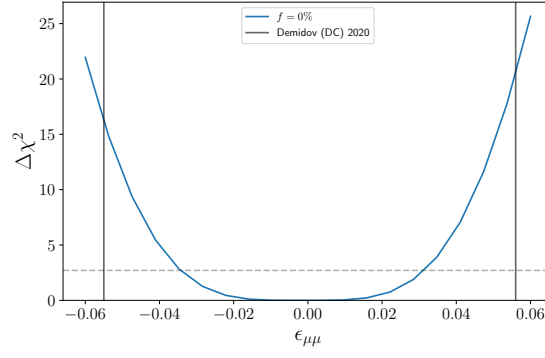


FIG. 4. Expected pulls of predicted event numbers for PINGU. We compare the NSI event count with $\epsilon_{\mu\tau} = -0.05$ to the standard interaction count

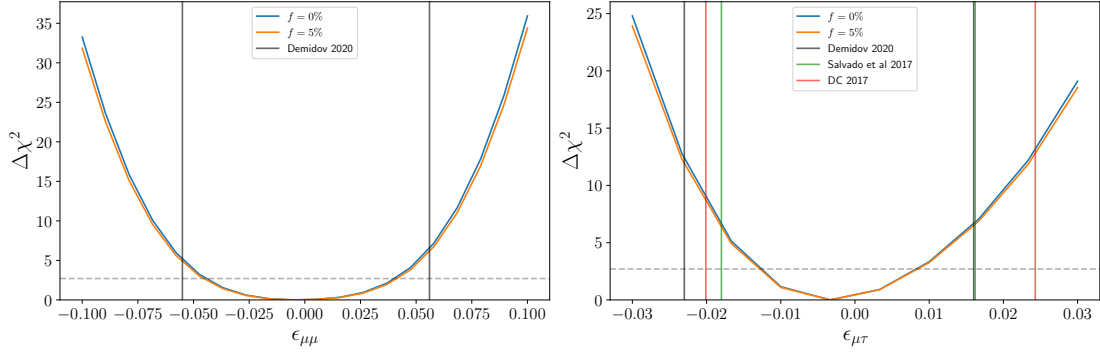


FIG. 5. Confidence levels from this analysis on the NSI parameters for systematic error and without. The black lines show the 90% credibility region from [11].

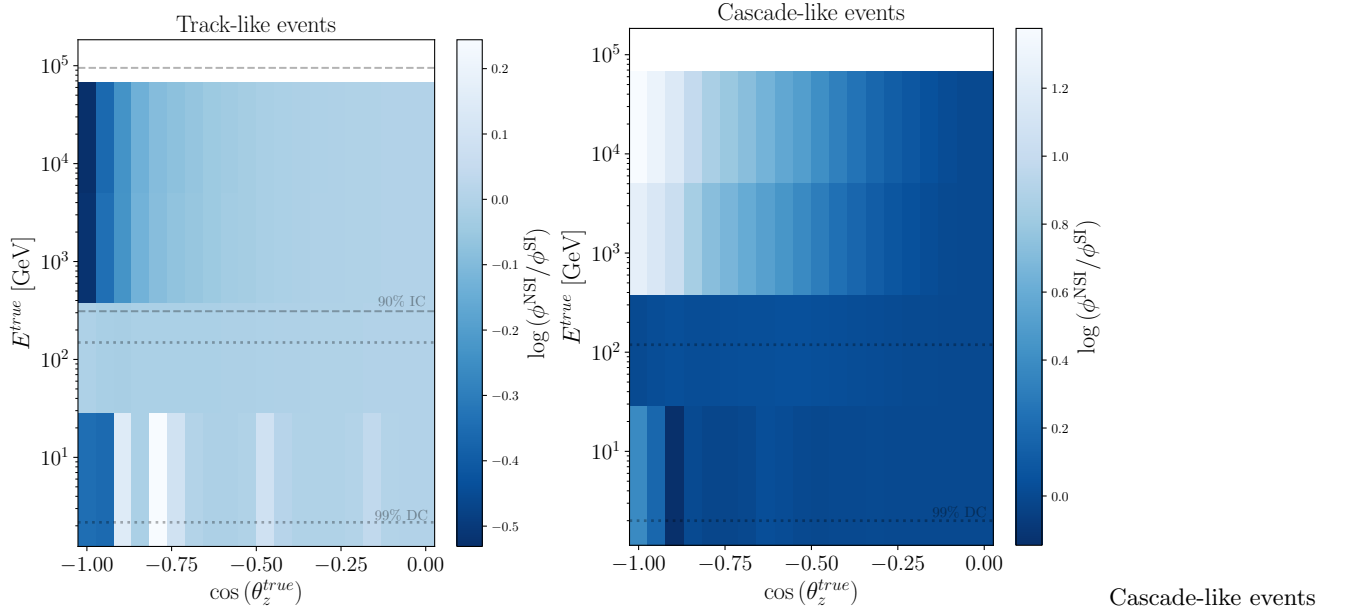


FIG. 6. Ratio of detector level NSI to SI $\nu_\mu + \bar{\nu}_\mu$ fluxes. Dotted (dashed) lines show the region in which 90% of the DeepCore/PINGU (IceCube) data are contained

- [2] A. M. Dziewonski and D. L. Anderson, Preliminary reference Earth model 25 (4) 297–356. doi:10.1016/0031-9201(81)90046-7.
- [3] IceCube Collaboration, All-sky point-source IceCube data: Years 2010-2012. doi:10.21234/B4F04V.
- [4] IceCube Collaboration, Search for sterile neutrinos with one year of IceCube data.
URL <https://icecube.wisc.edu/data-releases/2016/06/search-for-sterile-neutrinos-with-one-year-of-icecube-data/>
- [5] M. G. Aartsen et al., Searching for eV-scale sterile neutrinos with eight years of atmospheric neutrinos at the IceCube Neutrino Telescope 102 (5) 052009. doi:10.1103/PhysRevD.102.052009.
- [6] IceCube Collaboration, Three-year high-statistics neutrino oscillation samples. doi:10.21234/ac23-ra43.
- [7] IceCube Collaboration et al., Measurement of Atmospheric Neutrino Oscillations at 6–56 GeV with IceCube DeepCore 120 (7) 071801. doi:10.1103/PhysRevLett.120.071801.
- [8] IceCube Collaboration 1 et al., Measurement of atmospheric tau neutrino appearance with IceCube DeepCore 99 (3) 032007. doi:10.1103/PhysRevD.99.032007.
- [9] I. Esteban et al., The fate of hints: Updated global analysis of three-flavor neutrino oscillations 2020 (9) 178. doi:10.1007/JHEP09(2020)178.
- [10] IceCube Collaboration, IceCube Upgrade Neutrino Monte Carlo Simulation. doi:10.21234/qfz1-yh02.
- [11] Bounds on non-standard interactions of neutrinos from IceCube DeepCore data - INSPIRE.
URL <https://inspirehep.net/literature/1769239>
- [12] M. Maltoni and T. Schwetz, Testing the statistical compatibility of independent data sets 68 (3) 033020. arXiv:hep-ph/0304176, doi:10.1103/PhysRevD.68.033020.